NUMERICAL SIMULATION OF PARTICLES DISPERSION AND DEPOSITION IN CHANNEL FLOW OVER TWO SQUARE CYLINDERS IN TANDEM

UDC 54-138 : 519.872

Abouzar Moshfegh[1], Mousa Farhadi[2]

[1]Faculty of Mechanical Engineering, Noshirvani University of Technology,
Babol, Islamic Republic of Iran
[2]Faculty of Mechanical Engineering, Noshirvani University of Technology, P.O.Box 484
Babol, Islamic Republic of Iran
E-mail: mfarhadi@nit.ac.ir

Abstract. *Numerical simulation of dispersion and deposition of aerosol particles in a channel flow over two square cylinders in tandem are studied. A Lagrangian particle tracking computational procedure was developed and was used for simulating particles transport and deposition. Drag, gravity and buoyancy effects are included in the computational model. Ensembles of particles in asterisk arrangement are released from different source points to calculate their capture efficiency on walls and obstructions. The changes in location of source points, gravity direction, size and density of particles and the gap between obstructions to reduce capture efficiency are discussed. Parallel time evolution of four different clusters of particles representing the worst possible situation, issuing from maximum obstruction capture efficiency, are illustrated.*

Key Words: *Obstructed Channel Flow, Lagrangian Tracking Procedure, Particle Dispersion and Deposition, Capture Efficiency*

1. INTRODUCTION

Experimental and computational studies of dispersion and deposition of aerosols due to its industrial and environmental significances, have received considerable attention in the recent years by a number of authors. An extensive review of particle diffusion in laminar flows was provided by Levich (1972). A simplified procedure for deposition and dispersion of suspended small particles was developed by Li et al. (1994).This approach can be used for analyzing flows in complex region of practical engineering interest. Dispersion of small particles in a numerically simulated random isotropic field was analyzed by Ounis and Ahmadi (1990). Sommerfeld and Qiu (1993) studied particle dispersion in a

---

confined swirling flow using numerical simulations and Phase-Doppler anemometry (PDA). One of the extensive reviews of the available experimental results was provided by McCoy and Hanratty (1977). Numerical simulations were performed for constant cross section duct flows and/or under laminar flow condition was investigated by others. May and Clifford (1967) examined the impaction of aerosol particles on cylinders, spheres, ribbons and discs experimentally.

The effect of obstructions on particles capture efficiency in a two stage electronic precipitator has been studied by Yong and Sang (1996). The particles deposition on a square cylinder placed in a channel flow was studied by Brandon et al. (2001) and the effects of Stokes and Reynolds numbers on particle trajectory and deposition were investigated. Barton (1995) described the results of a numerical simulation study concerning particle tracks over a backward facing step under laminar flow condition. Recently, the need of microelectronic and computer industries to control micro-contamination processes have generated considerable interest on the subject (Cooper (1986)). In particular, contamination has been identified as the major cause for loss of efficiency in manufacturing integrated-circuits microchips. Sommerfeld (1992) studied confined particulate two-phase flows including particle-wall collisions.

In this work, an infinitesimal velocity duct flow over two cylinders placed in tandem is studied elaborately. The useful numerical methods to solve the equation of motion for a Lagrangian particle tracking procedure are introduced. Transport of ensemble of particles with a diameter between 1 and 100 micron in asterisk deployment released from different source points, located in upstream of flow field are simulated. The effects of source point locations, diameter and density of particles, gravity and the gap between cylinders on total and obstruction capture efficiencies are investigated. Dust may accumulate on and around various components and connectors in electronic packages used in computer industry and cause a loss of yield in heat transfer and manufacturing. So, it seems to be desirable to understand the above-mentioned effects on particles deposition rate. Furthermore, it can provide an insight into the natural phenomena of sand dune formation and snow fences. The results show that a percentage of the released aerosols may deposit on cylinders due to impaction and interception.

2. MODELED FLOW FIELD AND NUMERICAL METHOD

Self-evident industrial applications of duct flows obstructed by different patterns of bluff bodies lead us to study such fluid flow fields herein, namely, the chimneys equipped with electrostatic precipitators to intercept passing pollutant particles from escaping hot gases, the fins, which are used for cooling two parallel electronic chipsets, and the heat exchangers devised for heating the air duct flow for air conditioning purposes. These are samples of aforesaid interest. The unsteady laminar flow over a square cylinder has been studied by a group of authors [12-16]. A similar case to the present square cylinders in tandem is also studied by Tatsutani, et al. (1993), Valencia (1998), Valencia and Paredesm (2003) and Farhadi et al. (2006).

Assuming an unsteady two-dimensional laminar field, a fully-developed regime at the channel inlet, and constant properties of fluid, the governing equations of flow field simulation including continuity and conservation of linear momentum are reduced to following dimensionless forms:

$$\frac{\partial u_i^*}{\partial x_i^*} = 0 \tag{1}$$

$$\frac{\partial u_i^*}{\partial t^*} + u_j^* \frac{\partial u_i^*}{\partial x_j^*} = -\frac{\partial p^*}{\partial x_i^*} + \frac{1}{Re} \frac{\partial^2 u_i^*}{\partial x_j^{*2}} \tag{2}$$

where u_i^* is the velocity, x_i^* is the position, t^* is the time, p^* is the pressure and Re is the Reynolds number of channel which is given by $Re = U_{max} H / v$

Where U_{max} is the maximum of parabolic velocity distribution at the channel inlet, H is the cylinders height and v refers to kinematic viscosity of fluid. Other dimensionless variables are defined as:

$$u_i^* = \frac{u_i}{U_{max}}, \ x_i^* = \frac{x_i}{H}, \ t^* = t\frac{U_{max}}{H}, \ p^* = \frac{p}{1/2\rho U_{max}^2} \tag{3}$$

Regarding Figure 1, the lengths of upstream and downstream of obstructions illustrated with L_u and L_d, were set equal to 5H and 29H, respectively. The blockage ratio (h/H) of channel is considered constant and equal to 12.5% in this simulation. A staggered non-uniform grid distribution was used for the present computation as velocity grid points are displaced comparing to the pressure nodes. The number of used grid points was set as 253×168 for blockage ratio of 12.5%. Conservation equations (1-2) were discretized using the finite volume method while the QUICK[1] scheme was applied to discretize the convective and diffusive fluxes in momentum equation. A third order Runga-Kutta algorithm was used for the time integration in conjunction with the classical correction method at each sub-step. The continuity equation (Eq. 1) and the pressure gradient term in momentum equation (Eq. 2) were treated implicitly, while the convective and diffusive terms were treated explicitly. This method which is called semi-implicit fractional step method provides an approach that does not use pressure in the predictor step as in the pressure corrector method (such as well-known SIMPLE family of algorithms). The linear system was solved by an efficient conjugate gradient method with preconditioning.
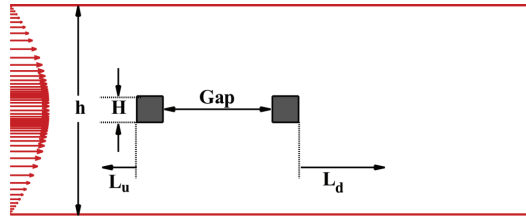

Fig. 1 Geometry of Problem

To examine the validity of the flow field simulator code, a graphical comparison with computed data by Breuer et al. (2000) for a duct flow obstructed by a single square cylinder was depicted. Fig. 2 shows the changes of Strouhal number with the channel Reynolds number was used as a bench mark for code verification, and reasonable agreement was achieved. Fig. 3 shows time-averaged streamlines of flow over two square cylinders for different gaps.

---

[1] -QUICK (Quadratic Upwind Interpolation for Convective Kinematics Scheme)
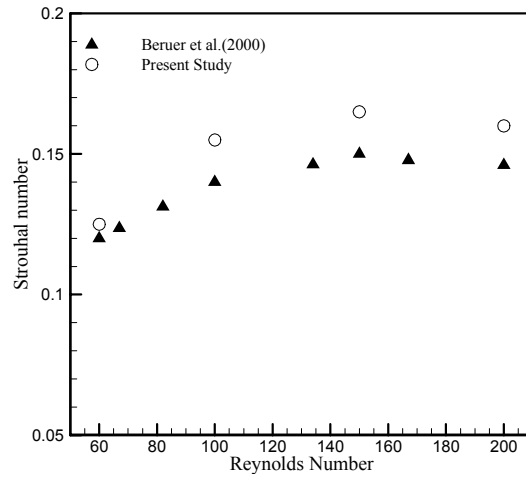
Fig. 2 Variations of Strouhal Number with Re Number
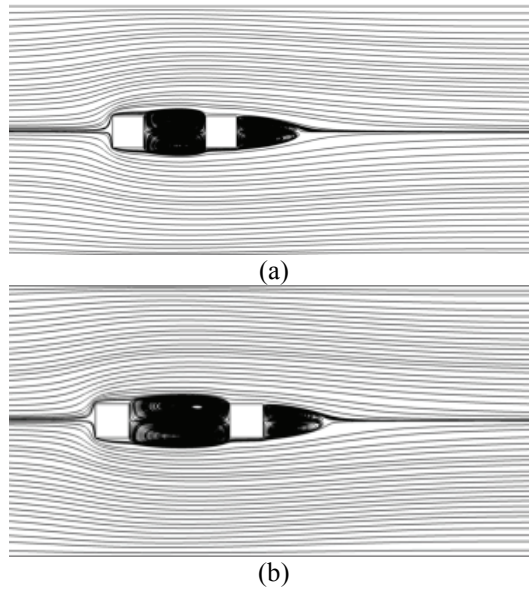for Duct Flow over a Single Square Cylinder

(a)

(b)
Fig. 3 Time-averaged Streamlines over Two Cubes
for (a) gap = 2 and (b) gap=3 at Re=100

3. PARTICLE EQUATION OF MOTION

Equation of motion of a small aerosol particle including nonlinear drag, gravity and Buoyancy effects with apparent mass is given by:

$$\frac{du_i^p}{dt} = \frac{3\mu^f\,Cdu_i^p\,Reu_i^p\,(u_i^f - u_i^p)\,Drag_i}{4\rho^p d^2(1 + 1/2S \times Buoyancy_i \times Gravity_i)C_c} +$$

$$\left(\frac{1 - 1/S \times Buoyancy_i \times Gravity_i}{1 + 1/2S \times Buoyancy_i \times Gravity_i}\right) \times g_i \times Gravit \qquad (4)$$

and

$$\frac{dx_i^p}{dt} = u_i^p \qquad (5)$$

Here, u^p_i is the velocity of the particle, x^p_i is its position, t is the time, g_i is the acceleration of body force (gravity), u^f is the local fluid velocity and S is the particle to fluid density ratio. Drag coefficient due to relative slip motion between particle and fluid which varies with the Reynolds number of particle. According to Hinds (1982), it is given respectively as:

$$Cdu^p = \frac{24}{Reu^p}\left(1 + \frac{3}{16}Reu^p\right) \quad \text{for} \quad 0 < Reu^p \le 0.5 - 1 \qquad (6)$$

and

$$Cdu^p = \frac{24}{Reu^p}\left(1 + \frac{1}{6}Reu^{p\,2/3}\right) \text{ for } 1 < Reu^p < 1000 \qquad (7)$$

Here, the Reynolds number of particle is determined by relative velocity between particle and fluid:

$$Reu^p = \frac{d\,|u^f - u^p|}{v^f} \qquad (8)$$

Where d is the particle diameter and v^f is the kinematic viscosity of fluid. In equation (4), C_c the Stokes-Cunningham correction factor for small particles is given by:

$$C_c = 1 + \frac{2\lambda}{d}[1.257 + 0.4\exp(-1.1d/2\lambda)] \qquad (9)$$

where λ is gas mean free path and is defined by:

$$\lambda(\mu m) = \frac{KT}{\sqrt{2}\pi d_m P} \qquad (10)$$

In this formulation, T and P are absolute temperature and pressure of gas respectively, d_m is gas molecular diameter and (K) is the Stephen-Boltzmann coefficient that is equal to 1.38×10^{-23} ($J/^\circ k$). Considering the configuration of given equation, drag, gravity and buoyancy refer to the effect of related forces on particle motion which are activated/deactivated by setting their values to 1 and 0 respectively.

Ounis and Ahmadi (1990) showed that other hydrodynamical forces such as the Basset history, the virtual mass, the pressure gradient and Faxen correction are much smaller than the drag force for small particles. For aerosols with the diameter between 1 and 100 micron like dust, fume, silt, cloud, fog, coal dust and bacteria these additional forces are

negligibly small. Therefore, they were not included in equation (4). For submicron particles Saffman lift force and Brownian motion must be considered. In the absence of Brownian motion the impaction is the dominant mechanism for deposition.

Most importantly, it is also assumed that the flow is highly dilute and the particles have no effect on the flow field and other particles. Furthermore, the compressibility and wall effects on drag coefficient are neglected. Furthermore, the rebound effect is neglected, so if any impaction to solid boundaries occurs, particle will stick to the surface till the end of the simulation process. The particles are assumed to be spherical, non-deformable, homogenous, neutral electrically, irrotational and with constant physical attributes. During Lagrangian particle tracking procedure, 'dt' refers to the lengths of time interval of numerical solution for each time step. In addition, the velocity and pressure values of flow field are interpolated by inverse distance weighting method for cell surrounding the particle at each time step.

4. RESULTS AND DISCUSSION

All investigations are executed for air in 298 °k with density of 1.171 Kg/m^3 and dynamic viscosity of 183.6e-7 $N.s/m^2$. It is also assumed that the gravity acceleration acting only along the (-y) and have a magnitude of 9.807m/s^2. The Stokes number (non-dimensional relaxation time) describes particle attributes and is defined as the ratio of particle stopping distance to the height of blocks.

$$Stk = \frac{\tau U_{max}}{H} \tag{11}$$

where τ is the particle response (relaxation) time defined as:

$$\tau = \frac{\rho^p d^2}{18\mu^f} \tag{12}$$

It is also assumed that there is no heat transfer between walls, obstructions and fluid.

Before any type of simulation of particles transport, the importance of different forces magnitude on particle motion must be examined perfectly. In the following discussion the industrial and environmental applications of aforesaid investigation to control the capture efficiency magnitude will be pointed out. During numerical solution, when we want to simulate several thousands of particles, vanishing of each term of equation of motion due to negligibility of related forces will considerably reduce the elapsed computation time. The effects of different compositions of forces exerted on the motion of a typical particle released motionless from $(x_0, y_0) = (-4.7, 0.9)$ are illustrated in Fig. 4. 'Dx' and 'Dy' which are (x) and (y) components of drag, 'G' that is Gravity and 'B' that represent buoyancy force, all acting on particle.

The horizontal and vertical motions of the particle are due to exertion of Dx and Dy respectively. (Dx+Dy), composition of two drag components, results in a middle trajectory with respect to Dx and Dy. Adding the gravity effect into (Dx+Dy), (Dx + Dy + G), leads to particle impaction onto the bottom wall of channel. Considering that Buoyancy always acts opposite to gravity, (Dx + Dy + G + B) causes the particle fall in a further place. The difference between magnitude of gravity and buoyancy forces changes by variation of particle density. Because of (Dx+G+B), (Dy+G+B), (Dx+G), (Dy+G), (B+G) and (G) the particle will be fallen downward vertically. This is the result of given inertia to the particle by infinitesimal velocity of present flow field via only a drag component that cannot cover the effect of gravity.
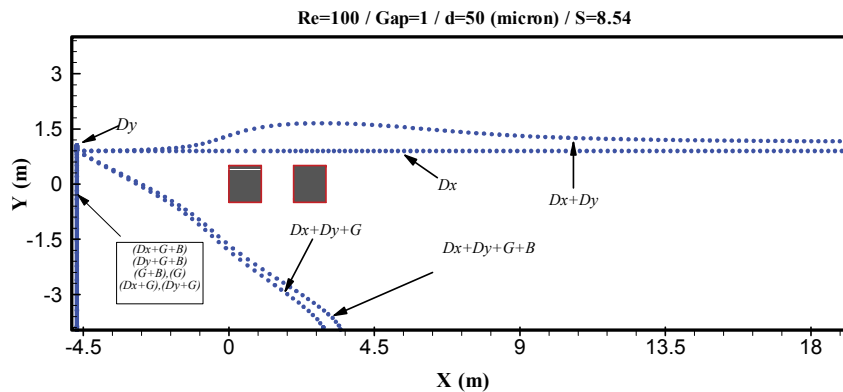
Re=100 / Gap=1 / d=50 (micron) / S=8.54

Fig. 4 Particle Trajectories due to Different Combinations of Forces

Finally, the effect of buoyancy force on particle motion is obviously negligible because of low density of the air with respect to the particle. All the illustrated trajectories vary by particle diameter and density changes, and what is discussed here cannot be considered as a rule. With the omission of the particle density effect, the particle moves in the streamline direction (Fig. 5).
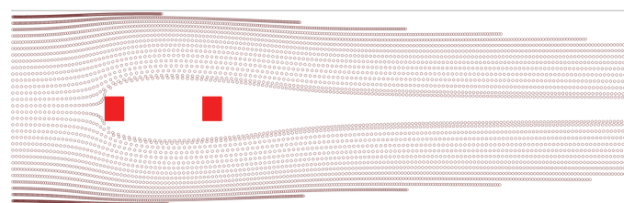

Fig. 5 Particle Trajectory for Particle Density Equal to Fluid

The sensitivity of falling of a 50 micron particle with respect to its density variations is illustrated in Fig. 6. For particles with (S<1), the buoyancy force magnitude will dominate the gravity force thus causing an impact upon the upper wall. Each trajectory represents densities 0.01, 0.05, 0.1, 0.5, 1.0, 1.171, 1.5, 2.25, 3.0, 3.75, 5.0, 10, 15, 25, 40, 65 (kg/m^3), respectively.

The above-mentioned sensitivity is highly dependant on particle mass as the heavy particles fall quicker than the lighter ones which can reach the channel outlet. Computation can be continued for a wide range of diameters while keeping the density constant. So, the particle trajectories describing falling sensitivity to diameter changes for different particle densities might be useful. What is concluded from these gathered range of diameters and densities and trajectories, showing falling sensitivity of particles, will help us to plot the capture efficiency diagrams in effective and accurate diameter and density intervals. This type of investigation is always recommended before starting your study based on an inaccurate range of particle densities and diameters. To predict particle depositions in different states of studied problem, the number of 205 particles arranged in asterisk arrangement are released motionless from a source point located at (x, y) = (-4, 0.5).

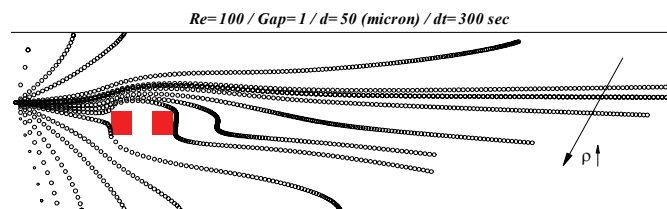*Re = 100 / Gap = 1 / d = 50 (micron) / dt= 300 sec*

Fig. 6 Falling Sensitivity to Density Changes

Simulation was iterated for the efficient diameter and density ranges, and the gap between cylinders. Finally obstruction capture efficiency (η_{obs}) and total capture efficiency (η_{tot}) were plotted for all situations. These parameters are defined as:

$$\eta_{obs} = \frac{N_{obs}}{N_{tot}} \quad\quad\quad (13)$$

$$\eta_{tot} = \frac{N_{dep}}{N_{tot}} \quad\quad\quad (14)$$

Where N_{obs} is the number of deposited particles on obstructions, N_{tot} is the total number of particles, and N_{dep} represents total number of deposited particles on both obstructions and channel walls. Fig. 7 illustrates total and obstruction capture efficiencies for an efficient range of densities and diameters which is computed according to aforesaid recommendation.

Each point represents efficiency values for an asterisk arrangement of 205 particles released as mentioned previously. Joint point of two groups of diagrams at zero efficiency point which are computed at the same density to fluid, means that the particles are moving approximately on streamlines. So, any changes in diameter or density of particles lead to trajectory deviation from flow streamlines until total capture efficiency is equal to 1.0 and then all the particles fall. Moreover, mass of particle which is given by $m = \pi d^3 \rho^p / 6$ which varies by third order of diameter and first order of density. So, the diameter changing effect is superior to some factors like mass increment and falling of particles. Thus the range of density variations is drastically limited by increment of diameter. Increasing trend of total capture efficiency diagrams implies a direct relationship between mass and unsuccessful transport of particles to the channel outlet. The gap distance between two cylinders has no any considerable effect on capture efficiency values.

In some industrial and environmental applications, the percent of deposited particles on walls and obstructions play a prominent role during designing procedure. Therefore, the extreme point of obstruction capture efficiency diagrams can be considered as a critical point; it leads us to optimize the system. Let the present problem as an approximation of a bundle of cylindrical heater elements be devised in a channel to heat the air (gas) moving over them, or cylindrical fins be placed vertically between two parallel flat plates (Electronic chipsets as an example) for heat transferring purposes. For increasing the rate of heat transfer from obstructions some elements must be considered during diagram interpretations. For example the thermal attributes (conductivity, being-vaporizable, etc.) of sedimentary particles, the rate of particle propagations and depositions, the pattern of their settlement on obstructions, etc. are notable. To interpret only on the basis of particle conductivity, the filtering process at the channel inlet must excuse the particles having the correspondent range of diameters and densities to what that is attained from minimum values of η_{obs} for nonconductor particles and maximum values of η_{obs} for conductor particles. The changes of gap distance between two cylinders have a slight effect on efficiency values due to tandem arrangement of cylinders.

Fig. 8 illustrates the parallel time evolution of 820 particle transports arranged in an asterisk form (Radius = 0.5) centered at entrance $(x,y) = (-4, 0.5)$ and released initially motionless with different diameters and densities according to Table 1. Each point identifies the location of one particle. High values of total elapsed time for particle transports imply the infinitesimal given inertia by flow field to the particles. If the source point were located on symmetry line of the channel, the values of capture efficiencies for both directions (y & -y) of gravity acceleration would be equal because of having an axisymmetric flow field. Also, the mentioned equality of capture efficiencies is established for two source points having the same distance from the

centerline while the upper source is subjected to the gravity acceleration along direction (-y) and the down one is subjected to the gravity along direction (y). Demonstration of a typical parallel time evolution of particle dispersions and depositions in extreme point were depicted on the basis of the nearest points instead. Table 1 contains the attributes of four different clusters of particles with each one referring to a maximum value of η_{obs} at sub diagrams of Fig. 7.
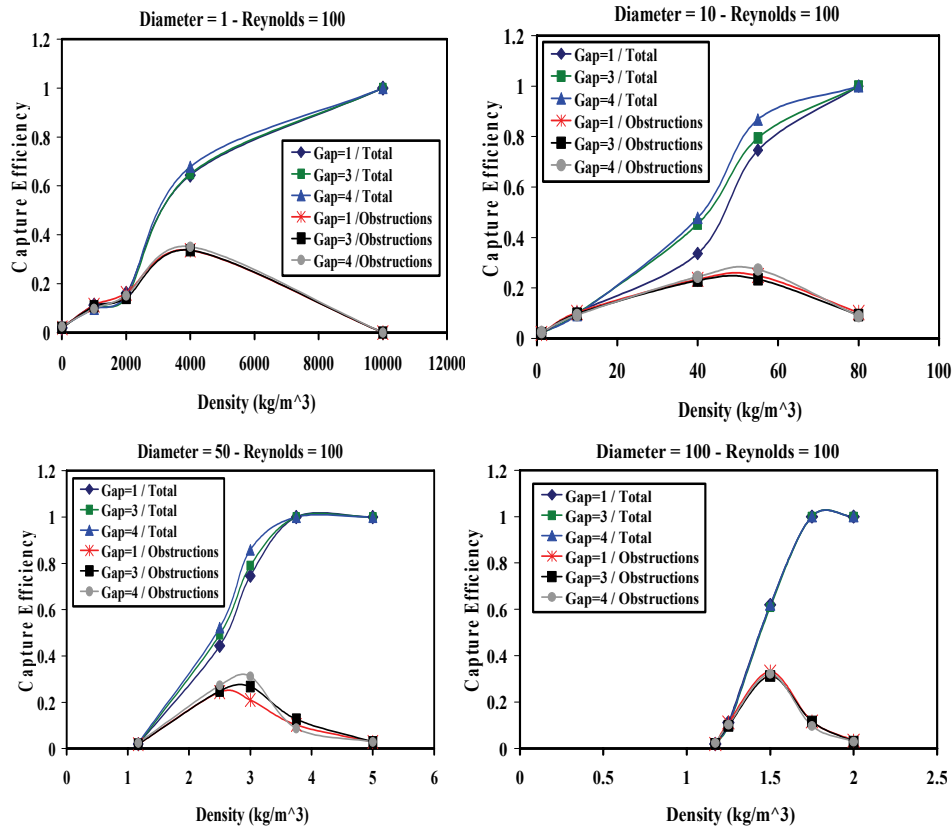

Fig. 7 Total and Obstructions Capture Efficiency of Four Different Particle Diameters at Re = 100 and Varying Gaps

Table 1 Released Particles Clusters Characteristics

	Cluster1	Cluster2	Cluster3	Cluster4	Total
Number of Particles	205	205	205	205	820
Diameter (m^2)	1	10	50	100	-
Density (kg/m^3)	4000	55	3	1.5	-
Stk .10^6	0.0189	0.0261	0.0356	0.0712	-
shape	◊	Δ	□	○	-
Total Time Steps	181	165	181	173	-
η_{obs}	0.3512	0.2731	0.3122	0.3219	0.3146
η_{tot}	0.6781	0.8683	0.8585	0.6195	0.7561

Re=100 / Gap=4 / dt=250sec / Time Step=0

Re=100 / Gap=4 / dt=250sec / Time Step=17

Time Step=30

Time Step=52

Time Step=89

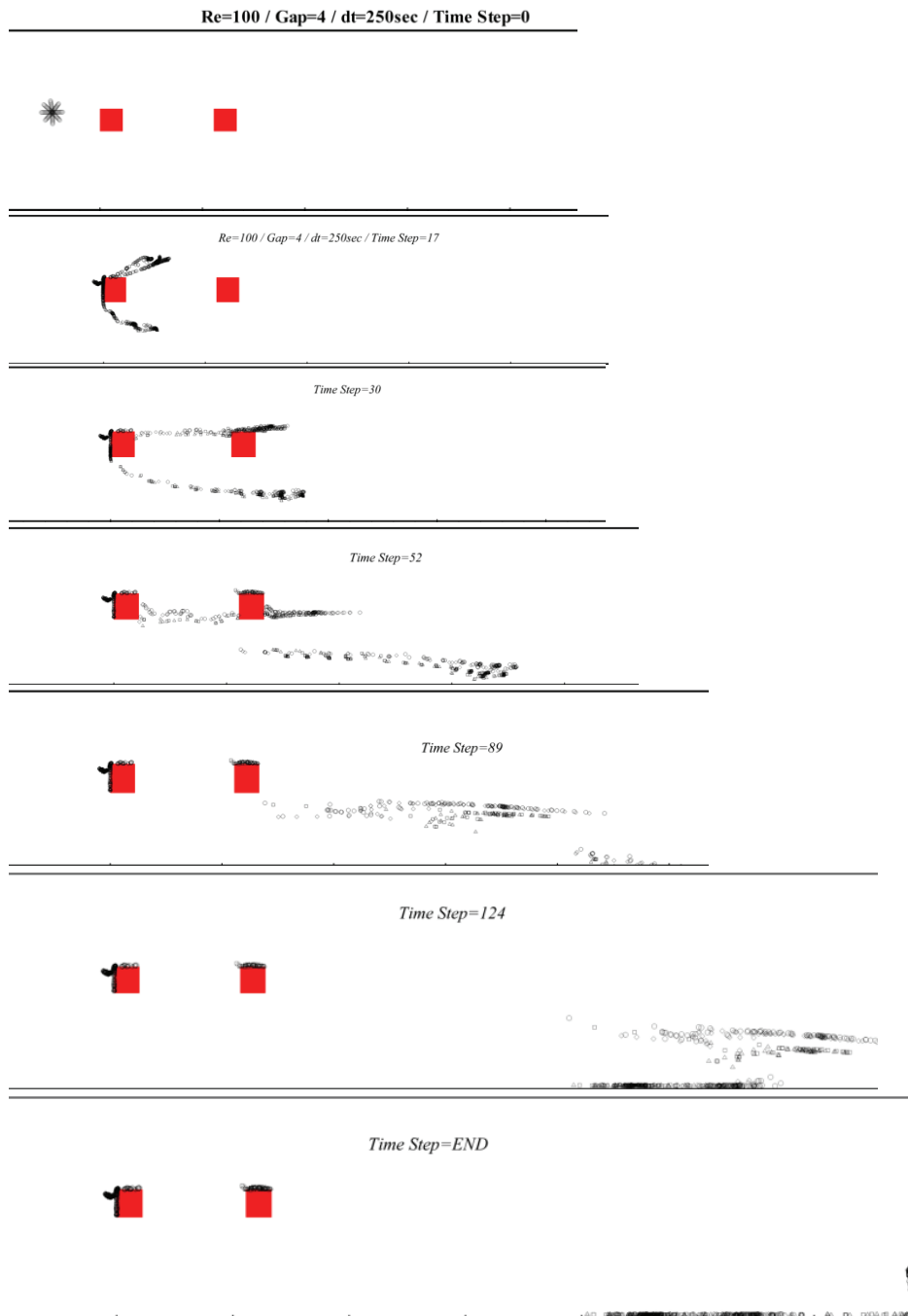*Time Step=124*

Time Step=END

Fig. 8 Parallel Time Evolution of Four Different Clusters of Particles
Released Motionless from a Source Point

They are selected here to demonstrate the quality of dispersion and deposition of the worst possible situation (maximum obstruction capture efficiency) in the present problem. It is assumed that a particle does not affect the motion of other ones and *vice versa*. So animating the particle transports and calculating their capture efficiencies using superposition principle is a reasonable decision.

5. CONCLUSION

In this paper, a digital simulation method using a Lagrangian tracking procedure was adopted to analyze the quality of dispersion and deposition of aerosol particles ($1<d<100$ micron). Weight of different forces acting on a particle with Stk=1.186e-07 and falling sensitivity to density changes for a 50 micron ($1.186e-10<Stk<7.709e-07$) were studied. Capture efficiency diagrams were plotted for ensemble of 820 particles with different Stokes numbers and the effects of diameter, density, gravity orientation, source point locations and the gap between two cylinders were discussed. On the basis of the results presented, the following conclusions are drawn:

• In low Reynolds numbers, the drag force exerted by the main flow could not cover the gravity effect on particle motion as the particle' falling takes place,

• The effect of buoyancy force on particle motion is obviously negligible because of low density of the air with respect to the particle,

• Having full-detailed data of diameter and density of involving aerosol particles in simulation is a prerequisite to plot capture efficiency values,

• Diameter changing effect is dominant to mass increment and falling of particles. Finally, the range of density variations is drastically limited by diameter increment,

• The gap distance between two square cylinders has no considerable effect on capture efficiency values,

• Intervals of extreme efficiency values attained from related diagrams lead us to control particle deposition rates on obstructions with respect to their attributes and type of the under designing system.

REFERENCES

1. Barton, I. E., 1995, *Computation of Particle Tracks over a Backward-Facing Step*, Journal of Aerosol Science, 26(6) pp 883-901.
2. Brandon, D. J. and Aggarwal, S.K., 2001, *A Numerical Investigation of Particle Deposition on a Square Cylinder Placed in a Channel Flow*, Aerosol Science and Technology, 34(4) pp 340-352.
3. Breuer, M., Bernsdorf, J., Zeiser, T., Durst, F., 2000, *Accurate Computations of the Laminar Flow past Square Cylinder Based on Two Different Methods: Lattice-Boltzmann and Finite Volume*, Int. Journal of Heat and Fluid Flow, 21 pp 186-196.
4. Cooper, D. W., 1986, *Particulate Contamination and Microelectronics Manufacturing: an Introduction*, Aerosol Science and Technology, **5** pp 287-299.
5. Farhadi, M., Sedighi, K. and Madani, S. M., 2006, *Convective Cooling of Tandem Heated Squares in a Channel*, Proceedings of the 3rd BSME-ASME International Conference on Thermal Engineering, 20-22 December, Dhaka, Bangladesh.
6. Hinds, WC., 1982, *Aerosol technology, properties behavior, and measurement of airborne particles*, New York: John Wiley and Sons.
7. Levich,V.G., 1972, *Physicochemical Hydrodynamics*, Prentice-Hall, Englewood Clifts, NJ.

8.   Li A, Ahmadi G, Bayer RG., Gaynes MA, 1994, *Aerosol Particle Deposition in an Obstructed Turbulent Duct Flow*, Journal of Aerosol Science, 25 pp 91-112.
9.   May, K. R., and Clifford, R., 1976, *The Impaction of Aerosol Particles on Cylinder, Sphere, Ribbons and Disks*, Annals of Occupational Hygiene, 10 pp 83–95.
10. McCoy, D. D. and Hanratty, T. J., 1977, *Rate of Deposition of Droplets in Annular Two-Phase Flow*, Int. J. Multiphase Flow, 3 pp 319-331.
11. Okajima, A., 1999, *Strouhal Numbers of Rectangular Cylinders,* Journal of Fluid Mechanics, 123 pp 379-398.
12. Ounis, H., and Ahmadi, G., 1990, *Analysis of Dispersion of Small Spherical Particles in a Random Velocity Field*, Journal of Fluids Engineering, 112 pp 114-120.
13. Rahnama, M., Hashemian, S. M., Farhadi, M., 2005, *Forced Convection Heat Transfer from a Rectangular Cylinder: Effect of Aspect Ratio*, 16th International Symposium on Transport phenomena (ISTP-16), August 29 - September 1, Prague, Czech Republic.
14. Sharma, A., and Eswaran, V., 2004, *Heat and Fluid Flow Across a Square Cylinder in The Two-Dimensional Laminar Flow Regime,* Numerical Heat Transfer, *Part A*, 45 pp 247-269.
15. Sommerfeld, M. and Qiu, H. H., 1993, *Characterization of Particles-Laden Confined Swirling Flows by Phase-Doppler Anemometry and Numerical Calculation,* Int. J. Multiphase Flow, 19 pp 1093-1127.
16. Sommerfeld, M., 1992, *Modeling of Particle-Wall Collisions in Confined Gas - Particle Flows*, Int. Journal of Multiphase Flow, 18 pp 905-926.
17. Tatsutani, R., Devarakonda, R., Humphrey, J. A. C., 1993, *Unsteady Flow and Heat Transfer for Cylinder Pairs in a Channel*, Int. Journal of Heat and Mass Transfer, 36 pp 3311-3328.
18. Turki, S., Abbassi, H., and Ben Nasrallah, S., 2003, *Two-Dimensional Fluid Flow and Heat Transfer in a Channel with a Built-in Square Cylinder*, Int. Journal of Thermal Science, 42 pp 1105-1113.
19. Valencia, A., 1998, *Unsteady Flow and Heat Transfer in a Channel with a Built-in Tandem of Rectangular Cylinders*, Heat and Mass Transfer, 33 pp 465-470.
20. Valencia, A., Paredesm R., 2003, *Laminar Flow and Heat Transfer in Confined Channel Flow Past Square Bars Arranged Side by Side*, Heat and Mass Transfer, 39 pp 721-728.
21. Yong J.S. Sang S.K, 1996, *Effect of Obstructions on The Particle Collection Efficiency in a Two Stage Electrostatic Precipitator*, Journal of Aerosol Science, 27(1) pp 61-74.

NUMERIČKA SIMULACIJA RASIPANJA I TALOŽENJA ČESTICA U KANALSKOM TOKU IZNAD DVA KVADRATNA CILINDRA U PARU

Abouzar Moshfegh, Mousa Farhadi

Numerička rešenja rasipanja i taloženja aerosolnih čestica u jednom kanalnom toku iznad dva kvadratna cilindra u paru se proučavaju. Računska procedura praćenja lagranžovih čestica je razvijena i korišćena za simulaciju transporta i deponovanje čestica. Uticaji vučenja, gravitacije i potiska su uključeni u model računanja. Spojevi čestica u zvezdastom rasporedu se oslobađaju sa različitih izvornih tačaka kako bi se izračunala efikasnost njihovog hvatanja na zidove i prepreke. Takođe se razmatraju promene u lokaciji izvornih tačaka, pravca gravitacije, veličine i gustine čestica kao i jaz između prepreka radi umanjenja efikasnosti hvatanja čestica. Paralelno vreme razvoja četiri grupacije čestica koje predstavlja najgoru moguću situaciju uz maksimalnu opstrukciju efikasnosti hvatanja čestica takođe se ilustruje.

Ključne reči: *prepreečen kanalski tok, langražovski postupak praćenja, rasipanje i taloženje čestica, efikasnost hvatanja čestica*